Physica D 72 (1994) 324–342
North-Holland

SSDI 0167-2789(94)00004-A

PHYSICA D

Coupling induced statistical cycling in two diffusively coupled maps

Jérôme Losson [a] and Michael C. Mackey [b]

[a] *Department of Physics and Center for Nonlinear Dynamics, McGill University, 3655 Drummond, Montréal, Qc. H3G-1Y6, Canada*

[b] *Departments of Physiology and Physics, and Center for Nonlinear Dynamics, McGill University, 3655 Drummond, Montréal, Qc. H3G-1Y6, Canada*

Received 25 August 1993
Revised manuscript received 22 November 1993
Accepted 15 December 1993
Communicated by K. Kaneko

This paper discusses the effects of diffusively coupling two identical one dimensional maps. Attention is focused on situations where the local (isolated) maps are statistically stable, but where the coupled system is not. A biologically motivated map and the quadratic map are numerically shown to display this behavior. The piecewise linear tent map is then investigated analytically, and we give a phase diagram of this system which displays the location of nonequilibrium phase transitions. It is conjectured that the diffusive coupling of two chaotic but statistically stable maps (i.e. with asymptotically stable Perron–Frobenius operators) can yield a two-dimensional system which is not statistically stable, whose associated Perron–Frobenius operator is asymptotically periodic.

1. Introduction

In this paper, we examine phase transitions (defined in section 1.1 below) in two-dimensional maps obtained by diffusively coupling two identical one-dimensional chaotic maps. We discuss situations in which the statistical behavior of the decoupled maps is qualitatively different from that of the coupled system. The local maps are statistically stable, they possess an absolutely continuous invariant measure, and physical observables (the Boltzmann-Gibbs entropy, the mean activity, the autocorrelation function, etc,...) converge to a constant value in the asymptotic regime. The coupled maps, however, cycle statistically: the invariant measure is not reached asymptotically for almost all initial preparations, but instead a periodic cycle in density-space is reached (see the definitions of section 1.2). Physical observables in the latter situation are also seen to cycle periodically in the asymptotic regime, so that the thermodynamic equilibrium is in fact a sequence of metastable states visited periodically. Three systems are used to illustrate our discussion. The first is a biologically motivated map which is obtained from a model of neural activity framed as a differential delay equation. The other two are the celebrated quadratic map, and the generalized tent map, respectively. The latter is investigated analytically.

This work is motivated in part by the many investigations of coupled map systems known as coupled map lattices (CML's) [19,20], which are known to display a wide range of dynamical behaviors [5–7]. Statistical cycling has been numerically reported in the literature, mostly in cellular automata schemes [5,16] (although there is mention of numerical observations of this behavior in coupled map lattices

[4]). Houlrik's investigation of periodic symbolic orbits in two coupled Châté–Manneville maps [14] indicates that there is a underlying statistical periodicity. Previous investigations of two coupled maps, from different perspectives, include the works of Yamada and Fujisaka [32] (and references therein), Yuan et al. [18], Froyland [8] but these do not address the periodic statistical behavior reported here. The most striking observation is the possibility that large networks of elements with simple dynamics can display stable periodic statistical behavior [4,16]. There has been speculation in the literature concerning the possibility that such behavior be asymptotically observable in physical systems [16,27]. The results presented here show that statistical cycling can be explained analytically in a simplistic model, as be expected in more general settings: they clearly indicate the existence of complicated states of thermodynamic equilibria in the simplest CML (i.e. two elements). Discussion of this behavior in larger systems will be presented elsewhere, where we give sufficient analytic criteria for statistical cycling in classes of arbitrarily large (but finite) coupled map lattices [24].

In section 1.1, we introduce the three systems which will be discussed in this paper, as well as some of the ideas concerning the relation between phase space densities and thermodynamic states. In section 1.2, we formally define phase space densities, asymptotic stability and asymptotic periodicity.

In section 2.1, we relate discrete time maps to differential delay equations, and statistical cycling is discussed in section 2.2 for a biologically motivated map obtained from a differential delay equation. This behavior is studied numerically for the quadratic map in section 2.3.

In section 3, a detailed analytic and numerical investigation of the dynamics of two coupled generalized hat maps is presented. A phase diagram giving the *loci* in parameter space where phase transitions occur is described analytically in section 3.1, while section 3.2 illustrates the temporal evolution of a statistical quantifier, the Boltzmann–Gibbs entropy, when the underlying system is statistically periodic.

Section 4 presents a brief summary, and several conjectures concerning the Perron–Frobenius operator associated with the two-dimensional map are put forward.

1.1. Three simple maps

The two-dimensional maps considered here are constructed by diffusively coupling two one-dimensional maps:

$$\Phi \circ (x,y) = (x_1,y_1), \quad \text{with} \begin{cases} x_1 = (1-\varepsilon)S(x) + \varepsilon S(y), \\ y_1 = (1-\varepsilon)S(y) + \varepsilon S(x), \end{cases} \varepsilon \in [0,1], \tag{1}$$

where S denotes the local map. In this paper, we focus on three systems. One is the tent map rescaled so that it is onto $[0,1]$ independent of the parameter a:

$$S(z) = \begin{cases} az + 2 - a, & \text{if } z \in [0,(a-1)/a] \\ a(1-z), & \text{if } z \in [(a-1)/a,1] \end{cases} \quad \text{and } a \in (1,2]. \tag{2}$$

Another is obtained in section 2.1 by taking a singular perturbation limit on a differential delay equation to obtain

$$S(z) = \frac{az}{1+z^n}, \qquad a,\ n \in \mathbb{R}. \tag{3}$$

The third map is the celebrated quadratic map

$$S(z) = az(1-z), \quad a \in (1,4], \tag{4}$$

whose behavior reproduces that of the more realistic system (3), suggesting that the behavior discussed here may be generic in systems with a locally quadratic maximum.

Depending on the system's location in parameter space, the map (1) with nonlinearities (2), (3) or (4) transforms the unit square into a simply connected set (as shown in figs. 1a, 2a, 4b, for example) or a collection of disconnected sets (as in figs. 1b, 2b, 5b or 7). Here, we investigate the boundaries between regions in the (a, ε) plane[#1] in which the number of these sets differ. When the attractor is a simply connected set, ensemble statistics can be computed from a numerically obtained invariant measure to which almost all initial preparations evolve; we conjecture that this reflects a property of the associated Perron–Frobenius operator known as *asymptotic stability*. When the attractor is a collection of disconnected sets, almost all numerical initial conditions eventually reach a cycle in density space, and statistical quantities like the Boltzmann–Gibbs entropy, the temporal correlation function and more generally all ensemble averages are seen to cycle in the asymptotic regime with a period related to the number of disconnected sets forming the attractor. Such cyclical statistical behavior is well described for certain one-dimensional maps, and is conjectured here to reflect a property of the associated Perron–Frobenius operator known as *asymptotic periodicity* [21,26].

Before proceeding, let us clarify the link between phase transitions (i.e abrupt changes in the thermodynamic state of a system) and qualitative changes in statistical behavior (reflected by abrupt transitions in the number of disconnected sets forming the attractor). Consider the system $S_{\{\alpha\}} : \mathbb{X} \longmapsto \mathbb{X}$, parametrized by $\{\alpha\}$, a set of real parameters. $S_{\{\alpha\}}$ could be a map, a set of ordinary differential equation, or more generally any (semi)dynamical system, $\mathbb{X}$ being called the phase space (or state space) of $S_{\{\alpha\}}$.

The thermodynamic state of $S_{\{\alpha\}}$ is associated with a phase space density function[#2], $f_{\{\alpha\}} : \mathbb{X} \longmapsto \mathbb{R}$, which gives the probability that the system is at a given state $x \in \mathbb{X}$. When $f_{\{\alpha\}}$ changes abruptly as a result of changing the parameters $\{\alpha\}$, so does the thermodynamic state of $S_{\{\alpha\}}$ and the system undergoes a phase transition. The problem of identifying phase transitions is therefore reduced to that of finding the *loci* in parameter space where $f_{\{\alpha\}}$ changes abruptly. Such an abrupt change necessarily occurs when the number of sets on which $f_{\{\alpha\}}$ is nonzero changes (the union of these sets is called the *support* of $f_{\{\alpha\}}$). In the tent map example discussed below, the analytic criteria given for phase transitions are criteria for abrupt changes in the support of $f_{\{\alpha\}}$.

There are fundamental differences between the approach discussed here, and the usual discussion of the thermodynamics of dissipative dynamical systems. The most important is that the *thermodynamic formalism* introduced by Bowen [2], Ruelle [29], Sinai [30] and others (cf. [1] for a discussion of this formalism), which is the inspiration behind the existing studies of the thermodynamics of coupled map systems [3,11–13], makes use of symbols used to represent single trajectories, so that ensemble statistics on such systems are constructed as they would be for generalized interacting spin systems. The existence of such symbolic representations for the original dynamical system, and consequently the link with interacting lattice gas systems, is not the underlying premise here.

Let us now turn to some definitions necessary to formalize our presentation.

[#1] Note that the system is symmetric under the transformation $\varepsilon \leftrightarrow (1-\varepsilon)$, $S(x) \leftrightarrow S(y)$ so that we only consider the region of parameter space $0 \leq \varepsilon \leq 1/2$.

[#2] Actually, the thermodynamic state of $S_{\{\alpha\}}$ is equivalent to a measure space, and the measure space can be associated with phase space densities when certain conditions, which are met by the systems discussed in this work, are satisfied. For details, the interested reader is referred to [22].

1.2. Definitions

We first define what is meant by a phase space density, and then define the operator $\mathcal{P}_T$ induced by a transformation $T : \mathbb{X} \longmapsto \mathbb{X}$ which acts on these densities. Let the set of nonnegative elements of L^1 be denoted

$$L^1_+ = \{f \in L^1 : f(x) \geq 0 \text{ almost everywhere}\}$$

and the set of densities by

$$D = \left\{f \in L^1_+ : \|f\| = 1\right\},$$

where $\|\cdot\|$ denotes the L^1 norm:

$$\|f\| \equiv \int_{\mathbb{X}} |f(x)|\, dx = \int_{\mathbb{X}} f(x)\, dx$$

for densities.

The *Perron–Frobenius operator* $\mathcal{P}_T : D \longmapsto D$ is induced by measurable transformations T of the phase space $\mathbb{X}$ that are nonsingular. For any $f \in D$, the Perron–Frobenius operator is defined by

$$\int_A \mathcal{P}_T f \mu(dx) = \int_{T^{-1}(A)} f \mu(dx), \tag{5}$$

where $A \subset \mathbb{X}$ (and the measure μ is related to its density function f by the relation $\int_A f(x)\, dx = \mu(A)$). If the transformation T is the two-dimensional mapping Φ defined above and operating on $[0,1] \times [0,1]$, the generalization of (5) is

$$\mathcal{P}_\Phi f = \frac{\partial^2}{\partial x \partial y} \int_{\Phi^{-1}([0,x]\times[0,y])} \int f(u,v)\, dv\, du. \tag{6}$$

The operator $\mathcal{P}_T$ is called *asymptotically periodic* if there exist finitely many distinct functions $g_1, ..., g_a \in L^1_+$ with disjoint supports (i.e. $g_i(x) g_j(x) = 0$ for all x if $i \neq j$), a permutation α of the set $\{1, ..., r\}$ and positive continuous linear functionals $\lambda_1, ..., \lambda_r$ on L^1_+ such that

$$\lim_{n\to\infty} \left\| \mathcal{P}^n_T \left(f - \sum_{i=1}^{r} \lambda_i(f) g_i \right) \right\| = 0 \tag{7}$$

and

$$\mathcal{P}_T g_i = g_{\alpha(i)}, \quad i = 1, ..., r,$$

and *asymptotically stable* if it satisfies these conditions with $r = 1$.

In other words, the phase space density f of an AP system at any (large) time is a linear combination of "basis states" (denoted g_i above) with *disjoint* supports, and at every time step the coefficients

(λ_i) of this linear combination are permuted by α. Therefore, the density evolution in such systems is periodic, with a period ($\leq r!$) determined by the control parameters, but with the exact cycle depending on the initial preparation since the λ_i's are functions of the initial density. A direct consequence of asymptotic periodicity is that the thermodynamic equilibrium of the system consists in a sequence of metastable states which are visited periodically. This is reflected in the behavior of the Boltzmann–Gibbs entropy.

The Boltzmann–Gibbs entropy $\mathcal{S}$ of $f \in D$ is defined by

$$\mathcal{S}(f) = -\int_{\mathbb{X}} f(u)\log(f(u))\,\mathrm{d}u, \tag{8}$$

where f is the phase space density associated with a dynamical system operating in a phase space $\mathbb{X}$. When the system is in thermodynamic equilibrium, the Boltzmann–Gibbs entropy is usually thought of as being stationary at a local maximum (the internal energy being in a local minimum). The phase space density describing this equilibrium is a fixed point of the operator giving the evolution of densities (i.e. the Perron–Frobenius operator for discrete time maps, the Liouville (or Fokker-Planck) operator for deterministic (or stochastic) ODE's, etc,...). In contrast to the situation in which extensive quantities can be determined from the density of the invariant measure, the (most probable) state of thermodynamic equilibrium for an asymptotically periodic map is, as discussed above a collection of metastable states which are visited in alternation. Thus, the Boltzmann–Gibbs entropy in this metastable equilibrium oscillates periodically for almost all initial preparations:

$$\lim_{t^*\to\infty} \mathcal{S}(f^{t^*}) = \lim_{t^*\to\infty} \mathcal{S}(f^{t^*+\kappa}) \Longleftrightarrow \alpha^\kappa(i) = i \quad (i = 1,...,r) \quad \text{and} \quad \alpha^j(i) \neq \alpha^\kappa(i),\ j < \kappa. \tag{9}$$

To see this, note that $g_i = g_j$ a.e. $\Leftrightarrow i = j$ since two different g_i's have disjoint supports. In addition, recall that $\mathcal{P}g_i = g_{\alpha(i)}$ (with $i = 1,...,r$ and α a permutation of the set $\{1,...,r\}$), and therefore $f^{t^*} = \mathcal{P}^\kappa f^{t^*} \Leftrightarrow \alpha^\kappa(i) = i$. As a consequence, from (7), $f^{t_1} = f^{t_1+\nu}$ a.e. $\Leftrightarrow \nu = 0$ or $\alpha^\nu(i) = i$. Furthermore it is easy to show that if $f(x) = g(x)$ a.e., $\mathcal{S}(f) = \mathcal{S}(g)$ and hence

$$\lim_{t\to\infty} \mathcal{S}(f^t) = \lim_{t\to\infty} \mathcal{S}(f^{t+\nu}) \Longleftrightarrow f^t = f^{t+\nu},$$

with either $\nu = 0$ or ν such that $\alpha^\nu(i) = i$ which proves (9).

This cycling behavior of $\mathcal{S}$ is numerically illustrated in section 3.2 for the hat map, but is also observed in the sigmoidal map and the quadratic map.

2. Statistical cycling in the coupled maps

We now turn to a study of coupling induced statistical cycling in three systems. The first of these is obtained as the singular perturbation limit of a first order differential delay equation (DDE).

2.1. Delayed feedback control loops and one-dimensional maps

In this section we first quickly review the connection between continuous time models of delayed feedback control loops framed as DDE's and one-dimensional maps. We then discuss situations where coupling induced statistical cycling is observed in the two-dimensional system.

The DDE's considered are of the form

$$\frac{dx}{dt} = -\zeta x(t) + F(x(t-1)), \qquad \zeta \in \mathbb{R}^+, \quad t \geq 0, \tag{10}$$

with initial function $x(t) \equiv \varphi(t)$ for $t \in [-1,0]$ (the delay is, without loss of generality, rescaled to 1). Dividing by ζ and taking the limit $\zeta \to \infty$, $F/\zeta \to S$, one obtains from the DDE the difference equation

$$x(t) = S(x(t-1)), \quad t \geq 0,$$

with $x(t) \equiv \varphi(t)$, $t \in [-1,0)$. Confining our attention to integer values of time instead of a continuum, one obtains the one-dimensional map

$$x_{n+1} = S(x_n), \quad n \in \mathbb{N},$$

with x_0 given. The procedure outlined here is known as a *singular perturbation* of the map, and it has been extensively studied by Ivanov and Šarkovskiĭ [15], who have been able to show that certain dynamical properties of the map can be extended to the infinite dimensional continuous time DDE. We follow this procedure to obtain the nonlinearity (2) from a DDE known in the literature as the Mackey–Glass equation, proposed as an attempt to model oscillations in neutrophil counts observed in certain cases of chronic myelogenous leukemia [26]:

$$\frac{dx}{dt} = -\zeta x(t) + \frac{\tilde{a}x(t-1)}{1 + x^n(t-1)}. \tag{11}$$

Performing the singular perturbation procedure on (11) and setting $a = \lim_{\zeta \to \infty} \tilde{a}/\zeta$ yields the nonlinearity (2).

2.2. The sigmoidal map

Fig. 1 displays two projections of the phase space density on the $x - y$ plane which numerically illustrates the phenomenon we conjecture to be coupling-induced asymptotic periodicity.

The behavior displayed in fig. 1 can be summarized as follows: there are regions in the parameter space of system (1) with S given by (3) in which the individual maps are (numerically seen to be) statistically stable when they are decoupled (fig. 1a). When the coupling is turned on ($\varepsilon > 0$), phase space densities cycle periodically, and they are supported on disjoint subsets of the phase space (as shown in fig. 1b). Points belonging to one subset are mapped into another at the next time step and so on. The period of the cycle depends on the parameters a, n and ε, while the details of the asymptotic cycle (i.e. the fraction of points belonging to various subsets) depend on the initial distribution of (x,y) pairs (the support of the initial density). This behavior should be interpreted in light of our discussion on asymptotically periodic Perron–Frobenius operators (cf. section 1.1). We conjecture that fig. 1 illustrates coupling induced asymptotic periodicity of the Perron–Frobenius operator of Φ. If the coupling ε is increased further, the sets $\mathcal{B}$ and $\mathcal{D}$ of fig. 1 "break-up" (i.e. give rise to disconnected subsets) and the period of the density cycles increases. The dependence of this period on ε is complicated.

Before examining the analytically tractable tent map, we show that similar behavior is observed in coupled quadratic maps. This is interesting since it suggests that the behavior presented above is probably generic in maps with a locally quadratic maximum.

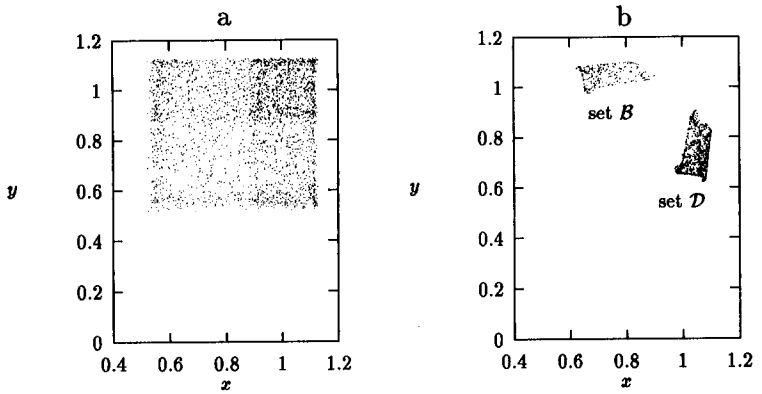

Fig. 1. Two-dimensional projection of the phase space density for the map (1) with nonlinearity (3) with $a = 1.65$ and $n = 8$ in both panels. Time $t = 6000$, the figure was made with 3500 points and the initial density was supported uniformly on $[0:1] \times [0:1]$. (a) $\varepsilon = 0.05$ and each map "fills" a simply connected subset of $\mathbb{R}^+$. The maps are conjectured to be asymptotically stable. (b) $\varepsilon = 0.05$ and for all initial $(x, y) \in \mathcal{B}$, we numerically observe that $\Phi(x, y) \in \mathcal{D}$ and points in $\mathcal{D}$ are mapped into $\mathcal{B}$. This is an example of coupling induced statistical cycling.

2.3. *The quadratic map*

The quadratic map is one of the most studied systems in the nonlinear dynamics literature. Here, we only review those aspects of its behavior connected with the presence of phase transitions. The main motivation for including this system in our discussion is that it reproduces most of the behavior displayed by the biologically motivated map of the previous example, while being much simpler analytically. The quadratic map is defined in (4) and its Perron–Frobenius operator $\mathcal{P}_q$ is

$$\mathcal{P}_q f(x) = \frac{1}{\sqrt{1 - 4x/a}} \left[f\left(\frac{1}{2} + \frac{1}{2}\sqrt{1 - \frac{4x}{a}}\right) + f\left(\frac{1}{2} - \frac{1}{2}\sqrt{1 - \frac{4x}{a}}\right) \right]. \tag{12}$$

When $a = 4$, the Perron–Frobenius operator is asymptotically stable, and the density of the invariant measure is

$$f^*(x) = \frac{1}{\pi\sqrt{x(1-x)}}.$$

This is the only value of a for which the invariant density is known, although the existence of absolutely continuous invariant measures has been proven for a belonging to sets of positive Lebesgue measure [17]. There is, in addition, a spectrum of values labeled a_n, $n = 1, 2, \ldots$, where so-called banded chaos has been reported numerically [23]. At these values, the behavior of the iterates of the map is very similar to those of the hat map when it is asymptotically periodic: the phase space densities oscillate periodically in time. At the value $a = a_n$, the period of the density cycle is 2^n. The recipe for finding the a_n's is given in [10]. A proof of the asymptotic periodicity of $\mathcal{P}_q$ at these values is not available yet, but the numerics clearly indicate that the so called "banded chaos" behavior in the quadratic map is in fact asymptotic periodicity [28].

The behavior shown in fig. 2 is the same as that found in the sigmoidal map. It is presented here to highlight the fact that coupling induced statistical cycling is probably a generic property of maps with

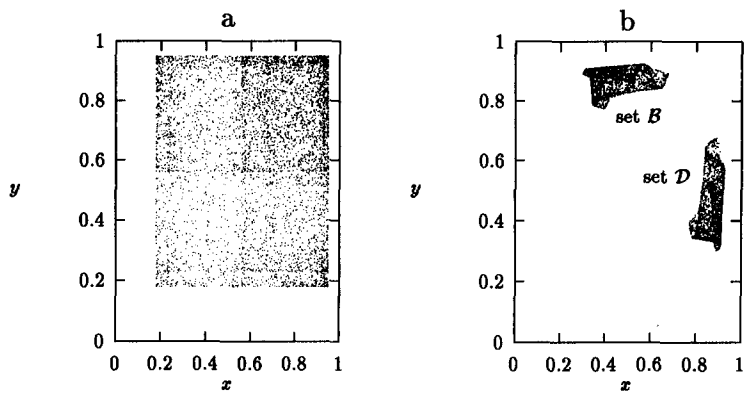

Fig. 2. Projection of the phase space density on the (x, y) plane for system (1) with the quadratic nonlinearity (4). In both panels, $a = 3.8$, time is $t = 6000$, the figure is made with 5000 pairs and the initial density was supported uniformly on $[0:1] \times [0:1]$. In (a) the maps are decoupled: $\varepsilon = 0$; numerical simulations indicate that the system is asymptotically stable. (b) $\varepsilon = 0.06$; the points in set $\mathcal{B}$ are mapped into set $\mathcal{D}$ and vice versa at every time step. This is clearly very similar to the behavior discussed in connection with the previous figure and is conjectured to reflect the underlying asymptotic periodicity of the Perron–Frobenius operator.

a quadratic maximum. In fact, it also observed in a simpler system, the generalized tent map, which is topologically conjugate to the quadratic map when $a = 2$, and which is analytically tractable.

3. Analytic investigation of two coupled tent maps

The one-dimensional semidynamical system known as the tent map (or hat map):

$$x_{n+1} = \begin{cases} ax_n, & \text{if } x_n \in [0, 1/2], \\ a(1 - x_n), & \text{if } x_n \in [1/2, 1], \end{cases} \tag{13}$$

where $a \in (1, 2]$ has been extensively studied during the past decade, in part because the Perron–Frobenius equation can be solved explicitly at different values of the parameter a [31,28]. The results which concern us here deal with the existence of critical values of the parameter a at which the thermodynamic state of (13) qualitatively changes. The Perron–Frobenius equation for the hat map (13) is

$$\mathcal{P}_h f(x) = \frac{1}{a}\left[f\left(\frac{x}{a}\right) + f\left(1 - \frac{x}{a}\right)\right], \tag{14}$$

where $f(x)$ is a phase space density for the system. Depending on the value of the parameter a, $\mathcal{P}_h$ can be proven to be either asymptotically stable or asymptotically periodic. To summarize its properties:

(i) $a = 2$. In this case $\mathcal{P}_h$ is asymptotically stable and the invariant density is the uniform density on the phase space $[0, 1]$. [It is easy to check that $1_{[0,1]}(x)$ satisfies (14)].

(ii) $a \in (\sqrt{2}, 2)$. $\mathcal{P}_h$ is asymptotically stable, and the invariant density is supported on a simply connected subset of $[0, 1]$.

(iii) $a \in (2^{1/2^{n+1}}, 2^{1/2^n})$, $n = 1, \ldots$. $\mathcal{P}_h$ is asymptotically periodic, and the period of the density cycle is 2^n. The activity is supported on the union of 2^n disjoint subsets $J_1, \ldots, J_{2^n}$, each J_i being the support of one of the g_i's defined in section 1.1.

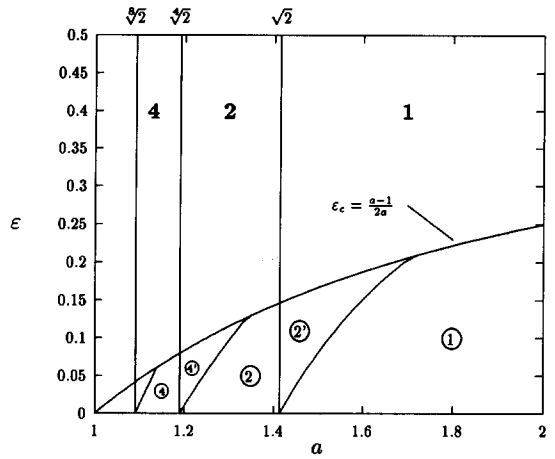

Fig. 3. Phase portrait of the map (1) with nonlinearity (2). In the upper regions labeled **1**, **2** and **4** the map is one-dimensional and respectively asymptotically stable (AS), asymptotically periodic with period 2 (AP-2) and period 4 (AP-4) (see figs. 4a,5a). In region ① (1) is AS but now both λ_1 and λ_2 are > 1 (see fig. 4b). In region ②' Φ is AP-2, but x and y are *out of phase* (see fig. 2e and the text for details). In region ② the map is AP-2, and x and y are either in phase or out of phase (see fig. 6a and the text for details). In regions ④ and ④' the map is AP-4. Details concerning these regions are described in the section entitled AP-4 (see fig. 7). In regions ②' and ④', the dynamics are not a trivial two-dimensional generalization of one-dimensional asymptotic periodicity, but rather *coupling induced.*

We want to investigate to what extent this structure of the dynamics of the hat map survives diffusive coupling. To that effect, the phase diagram in (a, ε)-space is discussed in section 3.1.

3.1. The phase diagram

The phase diagram of the two-dimensional system (1) with nonlinearity (2) naturally separates into two major regions: in the first, which corresponds in fig. 3 to those areas labeled with noncircled numbers, the behavior of Φ is effectively one-dimensional since the flow is contracted along one of the eigendirections. In the second, which encompasses the areas of fig. 3 labeled with circled numbers, the behavior is truly two-dimensional, since both eigendirections are unstable. The eigenvalues of the Jacobian of (1) with (2) satisfy the characteristic equation

$$[(1-\varepsilon)a - \lambda]^2 - a^2 = 0, \tag{15}$$

which has 2 solutions

$$\lambda_1 = a,$$

$$\lambda_2 = a(1-2\varepsilon). \tag{16}$$

When $\varepsilon \in ((a-1)/2a, (a+1)/2a)$, the dynamics are one-dimensional since in this case $|\lambda_1| > 1$ and $|\lambda_2| < 1$. The behavior of (1) matches exactly that of a single map and the upper portion of the phase diagram (fig. 3) describes the dynamics of (1).

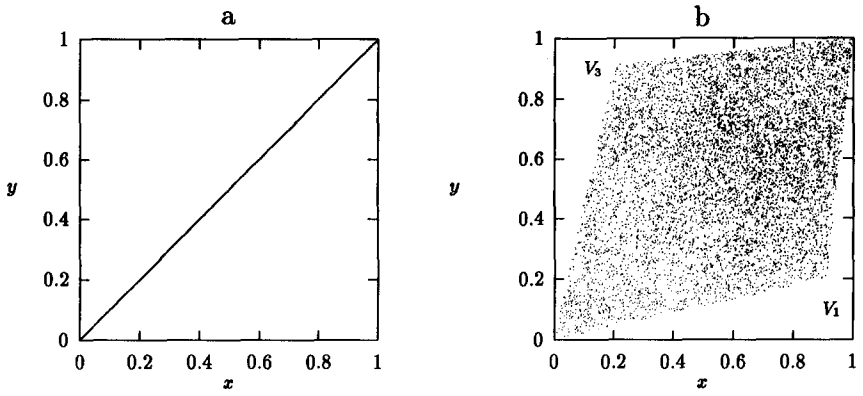

Fig. 4. Activity of the map Φ on the unit square. In (a), $a = 1.6$ and $\varepsilon = 0.35$ (system is in region **1**), hence $x = y$ eventually. In (b), $a = 1.7$, $\varepsilon = 0.1$ so the parameters are such that the map is in region ①. The vertices of the rhomboid are $V_0, \ldots, V_3$ given in (17). Both (a) and (b) were obtained numerically, using an ensemble of 8×10^3 initial conditions initially uniformly distributed on $[0,1] \times [0,1]$.

We therefore focus on the regions such that $\lambda_2 > 1$. These regions are below the critical line $\varepsilon_c = (a-1)/2a$ in fig. 3. The solid lines on fig. 3 bound regions in which the number of supports for the invariant density are fixed. We now describe each of these regions in detail.

3.1.1. Asymptotic stability

Regions in which Φ is AS are labeled with a ① and a "**1**" in fig. 3. In the region **1**, the dynamics are one-dimensional since one of the eigendirections is contracting (i.e. $|\lambda_2| < 1$) and the other is expanding ($\lambda_1 > 1$). In this region, Φ is asymptotically stable, and $x = y$: the behavior is that of a single asymptotically stable hat map. Fig. 4a displays the y vs x plot for 8×10^3 points after 50 time steps. Initially, these points were uniformly distributed on $[0:1] \times [0:1]$. The boundary between **1** and ② is the line $\varepsilon_c = (a-1)/2a$. The boundary between **1** and **2** is the value $a = \sqrt{2}$ (as in the one dimensional map). In the area labeled ①, the map is also AS, but now it is no longer effectively one-dimensional. The plot y vs x is given in fig. 4b, with the same initial conditions as in fig. 4a, but different ε. The coordinates of the vertices of the rhomboid are

$$
\begin{aligned}
V_0 &= (0,0),\\
V_1 &= \left(\left(1-\varepsilon+\frac{\varepsilon^2}{1-\varepsilon}\right)(2-a), 2\varepsilon(2-a)\right),\\
V_2 &= (1,1),\\
V_3 &= \left(2\varepsilon(2-a), \left(1-\varepsilon+\frac{\varepsilon^2}{1-\varepsilon}\right)(2-a)\right).
\end{aligned}
\tag{17}
$$

3.1.2. Asymptotic periodicity: AP-2

This behavior is observed in the three regions labeled **2**, ② and ②. In **2**, the behavior is again one-dimensional. The activity on $[0,1] \times [0,1]$ is plotted in fig. 5a, and is supported on two disjoint subsets of the diagonal $x = y$. The boundaries of this region are the value $a = \sqrt{2}$, the value $a = 2^{1/4}$ and the line $\varepsilon_c = (a-1)/2a$.

Region②

The boundaries of region ② are the line $\varepsilon_c = (a-1)/2a$, the value $a = \sqrt{2}$ and the line separating it from region ④, which will be discussed in section 3.1.3. For parameter values in ②, the behavior is statistically periodic with period 2: all points belonging to set $\mathcal{A}$ (in fig. 5b) at time t^* map into points belonging to $\mathcal{C}$ at time $t^* + 1$ and vice versa. This "flipping" behavior between two sets with disjoint supports, characteristic of asymptotic periodicity, is also observed for sets $\mathcal{B}$ and $\mathcal{D}$. Every point belonging initially to the unit square is asymptotically attracted to one of these four sets. Furthermore, the images of a point belong to $\mathcal{A} \bigcup \mathcal{C}$ or $\mathcal{B} \bigcup \mathcal{D}$, but do not flip between these. Schematically

$$\cdots \longmapsto \mathcal{A} \longmapsto \mathcal{C} \longmapsto \mathcal{A} \longmapsto \cdots$$
$$\cdots \longmapsto \mathcal{B} \longmapsto \mathcal{D} \longmapsto \mathcal{B} \longmapsto \cdots$$

The behavior observed in region ② is easily understood by noting that for such values of a the hat map is itself AP-2. The period 2 flipping described above therefore arises from the underlying asymptotic periodicity of the hat map. In other words, if ε were 0, one would obtain a picture rather close to that illustrated by fig. 5b (in fact, in that case, a y vs$x$ plot yields four square projection sets instead of the four rhomboids of fig. 5b). Cycle $(\mathcal{A}C\mathcal{A})$ can be called the *in phase* cycle, and the other, $(\mathcal{B}D\mathcal{B})$, *out of phase*. We will see later that the out of phase cycles can be stable in regions of parameter space where the in phase cycle is not. This is the origin of the coupling induced statistical periodicity observed in regions ② and ④. The activity observed in fig. 5b is sensitive to the initial distribution of points in the sense that if all initial points were included in the preimage of $\mathcal{A}$, all points would "flip" from set $\mathcal{A}$ to set $\mathcal{C}$ and back. Thus, the proportion of points which at time t^* are in set $\mathcal{A}$ depends in a sensitive way on the initial preparation. It is straightforward to derive analytic expressions for the edges of the four sets. For clarity, only the out of phase cycle is considered, and the expression for the coordinates of the edges of sets $\mathcal{B}$ and $\mathcal{D}$ are given in Appendix A (see also fig. 6b).

The region ②'

We now turn to the description of a novel type of dynamics, which is not a trivial two-dimensional generalization of the asymptotic periodicity well studied in 1-d maps. In region ②' the activity of the pair (x, y) can be described as asymptotic periodicity (although again this is an observation which does not stem from an investigation of the spectral decomposition of the 2-d Perron–Frobenius operator). The supports of the 2-d density on $[0{:}1]^2$ are disjoint as demonstrated in fig. 6a. These supports are symmetrical with respect to the $x = y$ line, and every point belonging to one support at time t^* belongs to the other at time $t^* + 1$ and vice versa. These supports form the *out of phase* cycle $\mathcal{B}D\mathcal{B}$ discussed previously, the *in phase* cycle $\mathcal{A}C\mathcal{A}$ now being unstable. Coordinates of the vertices of set $\mathcal{B}$ displayed in fig. 6b are given in Appendix A.

These vertices of $\mathcal{B}$ map onto the boundary of the set $\mathcal{D}$. When $\varepsilon = (a-1)/2a$, the critical value for which $\lambda_2 = 1$, the points β_0 through β_7 (and all the points in $\mathcal{B}$) collapse onto the single point with coordinates

$$\left(\frac{(a^2+1)}{a(a+1)}, \frac{(a-1)}{a}\right).$$

(Similarly, the points in $\mathcal{D}$ collapse onto its mirror image with respect to the $x = y$ axis, and the activity on $[0, 1] \times [0, 1]$ is then concentrated on the diagonal, as illustrated in fig. 5a.)

The condition on the parameters a and ε such that the set $\mathcal{B}$ maps into $\mathcal{D}$ and vice versa is obtained by performing a two-dimensional version of the calculation which yields the value $a = \sqrt{2}$ separating

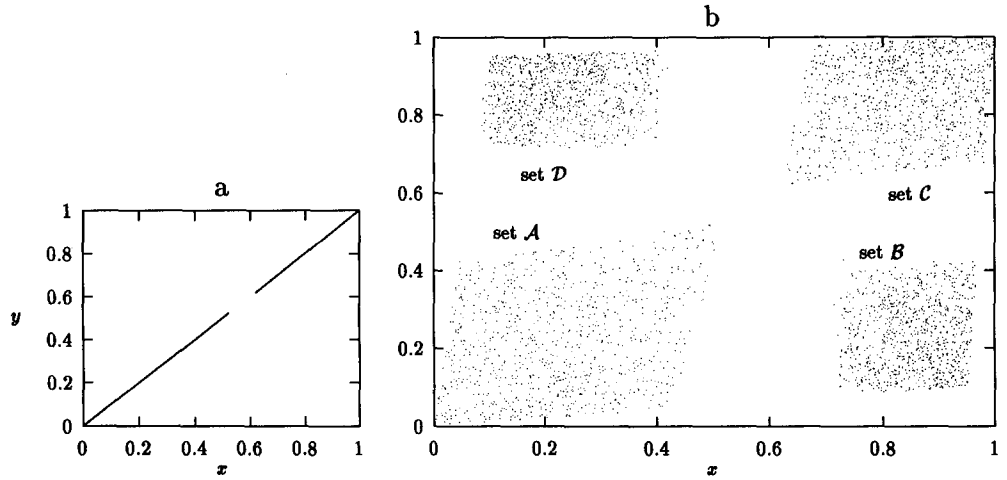

Fig. 5. Two-dimensional projection of the phase space density for two coupled tent maps at time $t = 6000$. The figure was made with 5000 points. In (a), $a = 1.38$ and $\varepsilon = 0.35$ (so (a, ε) is in region 2). All points on the left of the gap at time t^* are mapped into points on the right of the gap at time $t^* + 1$ and vice versa. In (b) $a = 1.38$ and $\varepsilon = 0.05$ (again (a, ε) is in region ②. All points in $\mathcal{A}$ at time t^* map into points belonging to $\mathcal{C}$ at time $t^* + 1$ and vice versa. This flipping also occurs for sets $\mathcal{B}$ and $\mathcal{D}$ (see text for details).

AP-2 and AP-4 in the one-dimensional hat map, given for example in [31,28]. The point whose image under Φ is the closest to the diagonal $x = y$ is β_1 (see fig. 6b). We call this image β_1^1. Its image under Φ, $\beta_1^2 = \Phi^2(\beta_1)$, lies within set $\mathcal{B}$ when the map is in region ②, i.e. when $\mathcal{B} \longmapsto \mathcal{D} \longmapsto \mathcal{B}$. When the map is in region ①, β_1^2 does not lie within set $\mathcal{B}$ but above the line segment $[\beta_5, \beta_6]$ (fig. 6 should prove useful to follow this geometrical digression). In other words, points which are in $\mathcal{B}$ do not necessarily return to $\mathcal{B}$ after two iterations under ②. Instead, they "fill up" the rhomboid displayed in fig. 4b. At the boundary between ① and ②, β_1^2 crosses the line segment $[\beta_5, \beta_6]$. Mathematically, this gives the following relation:

$$\Phi^2(\beta_1)^y = \beta_5^y,$$

or, explicitly,

$$[a(2\varepsilon - 1) + 1]\{a^3[4\varepsilon(\varepsilon - 1) + 1] + a^2[2\varepsilon(1 - 2\varepsilon)] - 2a[(1 - 2\varepsilon) + 1]\} = 0. \tag{18}$$

Eq. (18) can be solved for a as a function of ε analytically since it is a fourth order polynomial in a. We do not give the solution, but note that when $\varepsilon = 0$, the four solutions $a_{c,1,\ldots,4}$ are

$$a_{c,1} = 0, \quad a_{c,2} = 1, \quad a_{c,3,4} = \pm\sqrt{2}.$$

The root $a_{c,3} \equiv \sqrt{2}$ corresponds to the condition given by Provatas and Mackey for the one-dimensional case [28]. In addition, when $a \in [1, 2]$ all the roots are real. Two of these are irrelevant since they correspond to $\varepsilon \notin [0, 1]$ and the other two demarcate the region ② of fig. 3. Note that one of the roots coincides with the previously obtained condition $\varepsilon_c = (a - 1)/2a$ since

$$a_{c,2} = \frac{1}{1 - 2\varepsilon} \tag{19}$$

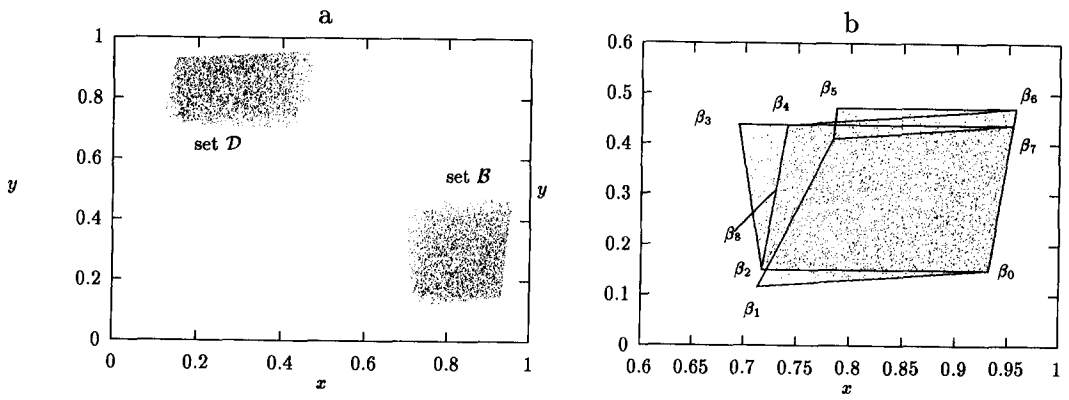

Fig. 6. Two-dimensional projection of the phase space density for two coupled tent maps at time $t = 6000$. The figure was obtained with 5000 points. (a) $a = 1.45$ and $\varepsilon = 0.075$ so the system is in region ②, with initial conditions uniformly distributed on $[0,1] \times [0,1]$. (b) The lines link the vertices given in eq. (A.1), Appendix A, plotted for $a = 1.45$ and $\varepsilon = 0.075$ superimposed with the data of panel (a).

is a solution of (18) for all a and ε.

The behavior illustrated in fig. 6 can be described as *coupling induced statistical cycling* since the individual maps are asymptotically stable when $(a, \varepsilon) \in$ ②. We conjecture that it reflects the asymptotic periodicity of the Perron–Frobenius operator for this system. A "period 4 version" of this phenomenon is observed numerically in ④, and is discussed in section 3.1.3.

3.1.3. Asymptotic periodicity: period 4

As in the one-dimensional case, there is period 4 statistical cycling in the coupled map system. The behavior in region ④ is illustrated in fig. 7.

It is possible to give an analytic expression for the boundary separating regions ② and ④. There are many different equivalent ways to obtain this expression, but each of these involves determining the conditions on a and ε such that points belonging to an element of a cycle (an "element" being one of the four disjoint sets forming a cycle) return to that element after 4 iterations under Φ. One point whose trajectory yields the desired critical condition has coordinates

$$\beta_8^x = \frac{\varepsilon(a-1)}{a(1-\varepsilon)} - \frac{4\varepsilon[1-a(1-\varepsilon^2)]-2+a}{1-\varepsilon},$$
$$\beta_8^y = \frac{a-1}{a}. \tag{20}$$

Following the images of this point under Φ, it can be shown geometrically that the condition analogous to (17) is given by

$$\Phi^3(\beta_8)^x = \Phi^8(\beta_8)^y, \tag{21}$$

which explicitly yields

$$a(2\varepsilon-1)\,[a(2\varepsilon-1)+1]\,\{a^7[16\varepsilon^4+12\varepsilon^2(1-2\varepsilon)-2\varepsilon]$$
$$+a^5[-8\varepsilon^2(1-\varepsilon)+2\varepsilon]+a^4[4\varepsilon(1-\varepsilon)-1]+2\}=0. \tag{22}$$

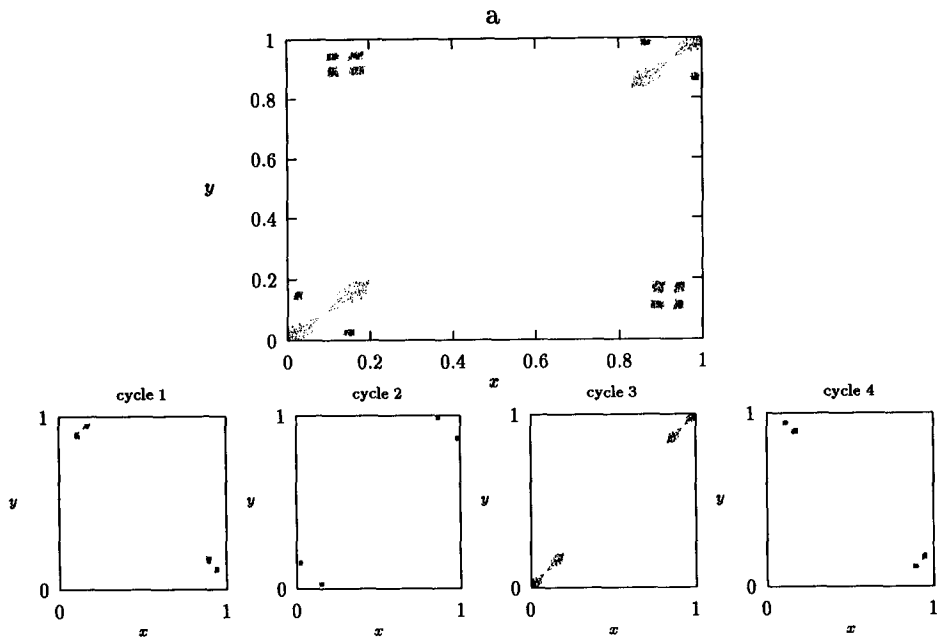

Fig. 7. Two-dimensional projection of the phase space density for two coupled tent maps. $a = 1.17$ and $\varepsilon = 0.05$ (i.e. the system is in region ④. The 16 disjoint supports shown in panel a) can be grouped into the four separate cycles of period 4 shown in the bottom panels. Points belonging to one cycle remain in this cycle. All points of the unit square eventually settle onto one of the cycles. The top panel was produced with 5000 pairs initially uniformly distributed in $[0,1] \times [0,1]$, and shows a snapshot of the activity at time $t = 200$. To obtain each of the four bottom panels, the initial points were uniformly distributed in a set belonging to one cycle, and each panel is the superimposition of four snapshots taken at four consecutive time steps $t = 200, \ldots, 203$.

The above is a ninth order polynomial in a. One of its roots is, as for condition (17),

$$a_{c,2} = \frac{1}{1-2\varepsilon}. \tag{23}$$

It is not possible to give the expression for the other roots but we note that at $\varepsilon = 0$, (22) becomes a sixth order polynomial with roots

$$a_{c,1,3} = \pm 2^{1/4}, \quad a_{c,4,5} = \pm i 2^{1/4}, \quad a_{c,5} = 1, \quad a_{c,6} = 0.$$

The root $2^{1/4}$ corresponds to the condition given in [28] for the one-dimensional transition between period 2 and period 4 asymptotic periodicity. The boundary between regions ② and ④, plotted in fig. 3, is the analytic curve $a_{c,1}(\varepsilon)$, determined from (22), for $\epsilon \in [0, 1/4]$.

In region ④, the in phase cycle (cycle 3 of fig. 7) disappears: this is analogous to the disappearance of the sets $\mathcal{A}$ and $\mathcal{C}$ (displayed in fig. 5) in region ②. The "period 8 version" of this phenomenon, as well as the boundary between period 4 and period 8 statistical cycling is discussed in Appendix B.

3.1.4. Asymptotic periodicity of higher period

We conclude the investigation of the phase diagram of the map Φ (fig. 3), by noting that one can numerically observe higher order bifurcations which correspond to the transitions from AP-8 to AP-16, and by conjecturing that transitions from asymptotic periodicity of period 2^n to asymptotic periodicity

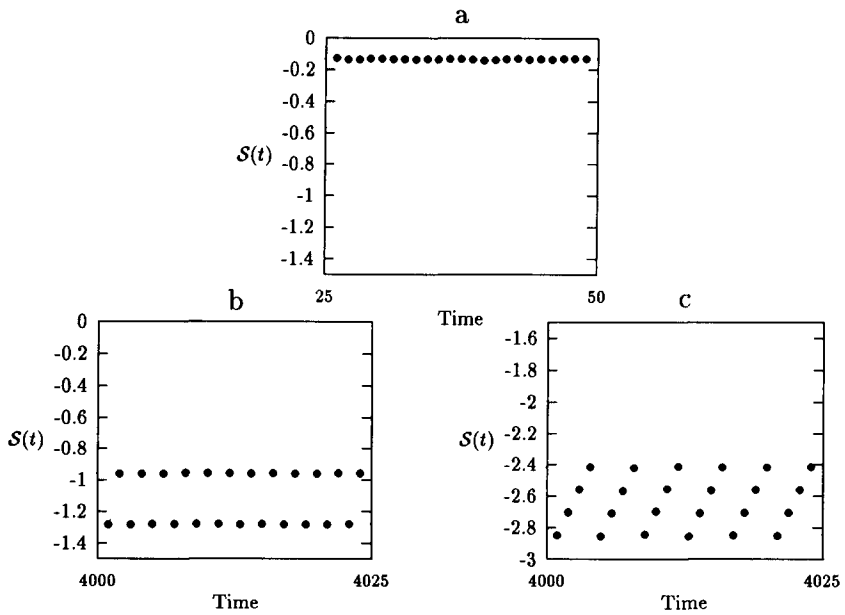

Fig. 8. Three types of asymptotic behavior of the Boltzmann–Gibbs entropy. (a) The map Φ is in region ①: $a = 1.85$, $\varepsilon = 0.1$. (b) The map Φ is in region ②: $a = 1.45$, $\varepsilon = 0.075$. (c) The map Φ is in region ④: $a = 1.16$, $\varepsilon = 0.05$. In all three cases, the initial values of x_1 and x_2 were uniformly distributed on the set $[0.3, 0.4] \times [0.8, 0.9]$.

of period 2^{n+1} can probably be observed for all n. In other words, numerical studies strongly suggest that the one-dimensional picture given in [28] essentially survives diffusive coupling, in the sense that there is a period doubling of the density cycles as the slope of the tent map is lowered from 2 to 1, but that it is modified by the appearance of coupling induced regions in which the behavior is not a straightforward generalization of the one-dimensional behavior (two of which, labeled ② and ④) are shown in fig. 3.

3.2. *On the evolution of statistical quantifiers*

In this section, the evolution of the Boltzmann–Gibbs entropy for the hat map is discussed in the various regions of parameter space. The purpose of this discussion is to illustrate the oscillatory behavior of statistical quantifiers, usually computed with the invariant density, when the underlying system is asymptotically periodic[#3].

The cycling displayed in fig. 8 is observed after transients were appropriately discarded: if the entropy behavior is seen to be the same for 10^4 time steps, then it is assumed that the asymptotic regime has been reached. In fig. 8a, the level reached by the entropy after about 10 iterations (for this particular initial condition) was the level at which the entropy was found after 10^4 iterations. The asymptotic cycling of S in figs. 8b and 8c, reflects the fact that the Boltzmann–Gibbs entropy is not the quantity to which the second law of thermodynamics applies for most asymptotically periodic system

[#3] The two coupled tent maps are not rigorously proven to be asymptotically periodic, but the analytical evidence provided in this paper strongly indicates that they are.

(or, more generally, for most dynamical systems). For a detailed discussion of the thermodynamics of asymptotically periodic systems, see [25].

4. Summary and conjectures

In this paper, we have numerically observed that for the sigmoidal map, and the quadratic map, the diffusive coupling of two chaotic but statistically stable elements can yield a system which shows periodic cycling of phase space densities, which we call "coupling induced statistical cycling". We conjecture that this behavior is a generic property of maps with a quadratic maximum.

We have constructed the analytic phase diagram for two diffusively coupled tent maps, which shows that the one-dimensional bifurcation structure of the Frobenius-Perron operator essentially survives diffusive coupling, modulo the appearance of regions in parameter space in which the behavior is not a straightforward two-dimensional generalization of the one-dimensional behavior. We conjecture that the two-dimensional Perron–Frobenius operator is asymptotically periodic when the one dimensional operator is, *but* that there are regions in parameter space in which the one-dimensional systems have asymptotic periods differing from the coupled system.

Finally, preliminary numerical results indicate that the statistical behavior discussed here is commonly observed in large (i.e. with more than 10^2 elements) lattices of diffusively coupled maps, whether the local dynamics be given by the piecewise linear tent map, or the smooth maps of section 2. There seem to be nontrivial correlations between the appearance of macroscopic large scale patterns in these lattices and statistical cycling. Such connections are presently under investigations, and will be reported elsewhere. In particular, it is possible to explain phase transitions in large lattices in terms of abrupt changes in the spectral properties of the Perron–Frobenius operator. The techniques used in this paper to describe asymptotic periodicity are not easily extendable to larger systems, because the geometrical insight is rapidly lost as the number of maps coupled together increases. However, the present results confirm the possiblity that asymptotic periodicity can be coupling-induced in simple maps, and as such have led to the use of general results from ergodic theory in higher dimensions [9] to describe asymptotic periodicity (and phase transitions) in large lattices [24]; the proper understanding of statistical cycling in large CML's is greatly facilitated by the present discussion of this behavior in the simplest possible CML.

5. Acknowledgements

We wish to thank the National Sciences and Engineering Research Council of Canada (NSERC), NATO for a collaborative research grant to M.C.M and FCAR for support to J.L. We also thank Danny Kaplan and Marc Courtemanche for helpful discussions.

Appendix A

The coordinates of the edges of the set B of figs. 5b and 6 are

$$\beta_0^x = \tfrac{(1-2\varepsilon+2\varepsilon^2)}{\varepsilon-1},$$

$$\beta_0^y = 2\varepsilon,$$

$$\beta_1^x = \tfrac{a(-1-a-4a^2\varepsilon+4\varepsilon^2a^2+4a\varepsilon+a^2-4\varepsilon^2a)(1-2\varepsilon+2\varepsilon^2)}{\varepsilon-1},$$

$$\beta_1^y = -2\varepsilon a\left(-1-a-4a^2\varepsilon+4\varepsilon^2a^2+4a\varepsilon+a^2-4\varepsilon^2a\right),$$

$$\beta_2^x = \tfrac{-4a\varepsilon-2+a+4\varepsilon^2a+4\varepsilon-2\varepsilon^2}{\varepsilon-1},$$

$$\beta_2^y = 2\varepsilon,$$

$$\beta_3^x = -\tfrac{2+3a\varepsilon-2\varepsilon^2a-4\varepsilon-a-8\varepsilon^4a^3-2\varepsilon^2a^2+a^2\varepsilon+2\varepsilon^2-a^4\varepsilon-12a^4\varepsilon^3+12\varepsilon^3a^3-6a^3\varepsilon^2}{\varepsilon-1},$$

$$-\tfrac{a^3\varepsilon+8a^4\varepsilon^4+6a^4\varepsilon^2}{\varepsilon-1},$$

$$\beta_3^y = a-2a\varepsilon-a^2+2a^2\varepsilon-a^3+6a^3\varepsilon-12a^3\varepsilon^2-6a^4\varepsilon+12a^4\varepsilon^2-8a^4\varepsilon^3+8\varepsilon^3a^3+a^4+2\varepsilon,$$

$$\beta_4^x = -\tfrac{3a\varepsilon+2-a-2\varepsilon^2a-4\varepsilon+2\varepsilon^2-4\varepsilon^2a^2+a^2\varepsilon+4\varepsilon^3a^2}{\varepsilon-1},$$

$$\beta_4^y = 2a\varepsilon-a-4a^2\varepsilon+a^2+4\varepsilon^2a^2+2\varepsilon,$$

$$\beta_5^x = \tfrac{a(-1-5a\varepsilon+8\varepsilon^2a+4a^2\varepsilon-4a^2\varepsilon^2+5\varepsilon+a-a^2-8\varepsilon^2-4\varepsilon^3a+a^4+16a^4\varepsilon^4-24a^3\varepsilon^2+24a^4\varepsilon^2)}{\varepsilon-1},$$

$$+\tfrac{a(32\varepsilon^3a^3+4\varepsilon^3+8a^3\varepsilon-32a^4\varepsilon^3-16\varepsilon^4a^3-a^3-8a^4\varepsilon)}{\varepsilon-1},$$

$$\beta_5^y = a(-1-4a\varepsilon+4\varepsilon^2a+4\varepsilon+a-4\varepsilon^2),$$

$$\beta_6^x = -\tfrac{(2\varepsilon-1)(2\varepsilon^2a^2-2\varepsilon^2a+a\varepsilon-a^2\varepsilon-1)}{\varepsilon-1},$$

$$\beta_6^y = \left(-1-4a\varepsilon+4\varepsilon^2a+4\varepsilon+a-4\varepsilon^2\right)a,$$

$$\beta_7^x = -\tfrac{1-2\varepsilon+2\varepsilon^2-a\varepsilon+2\varepsilon^2a-4\varepsilon^2a^2+a^2\varepsilon+4\varepsilon^3a^2}{\varepsilon-1},$$

$$\beta_7^y = 2a\varepsilon-a-4a^2\varepsilon+a^2+4\varepsilon^2a^2+2\varepsilon. \tag{A.1}$$

These coordinates are obtained by forward iterations of the four corners of the unit square under the action of the map Φ.

Appendix B

There is a region in parameter space in which the behavior is the period 8 analogue of that already described in regions ② and ④: the attractor on the unit square is a collection of 56 disjoint sets, forming 7 independent cycles of period 8 each[#4]. The boundary between region ⑧ and region ④ is given by the following criterion:

[#4] Since the behavior is period 8, one would expect 8 independent cycles yielding 64 disjoint supports, but one of these, the in phase cycle is not observed, an observation already in the period 2 and period 4 regimes.

$$\Phi^{13}(\beta_8)^x = \Phi^9(\beta_8)^x. \tag{B.1}$$

Mathematically, the condition is

$$\begin{aligned}&[a^2(2\varepsilon-1)+1][a(2\varepsilon-1)+1][a^{11}(256\varepsilon^8-896\varepsilon^7+1408\varepsilon^6-1280\varepsilon^5+736\varepsilon^4\\&-280\varepsilon^3+72\varepsilon^2-12\varepsilon+1)+a^8(-64\varepsilon^6+160\varepsilon^5-176\varepsilon^4+104\varepsilon^3-32\varepsilon^2+4\varepsilon)\\&+a^3(8\varepsilon^3-12\varepsilon^2+8\varepsilon-2)-2\varepsilon]=0.\end{aligned} \tag{B.2}$$

It is possible to factor the above polynomial into an eighth degree polynomial in ε and two monomials, so that two of the roots can be written explicitly:

$$a_{c,1}=\frac{1}{1-2\varepsilon},\quad a_{c,2}=\frac{1}{\sqrt{1-2\varepsilon}}. \tag{B.3}$$

The boundary drawn in fig. 1 between regions ⑧ and ⑧' shows $a_{\max}(\varepsilon)$ where $a_{\max}$ is the largest of the 12 other roots. When the coupling $\varepsilon = 0$, the 14 roots of the polynomial are:

$$\text{roots}: \pm 1,\ 1,\ 0,\ 0,\ 0,\ \pm 2^{1/8},\ 2^{1/8}(\tfrac{1}{2}2^{1/2} \pm i\tfrac{1}{2}2^{1/2}),\ 2^{1/8}(-\tfrac{1}{2}2^{1/2} \pm i\tfrac{1}{2}2^{1/2}),\ \pm i2^{1/8}.$$

The root $2^{1/8}$ corresponds to the condition given in [28] for the transition from period 4 to period 8 AP in the one-dimensional map.

References

[1] R. Badii, Conservation laws and thermodynamic formalism for dissipative dynamical systems, Riv. Nuov. Cim. 12 (1989) 1.
[2] R. Bowen, Markov partitions for Axiom A diffeomorphisms, Am. J. Math. 92 (1975) 725.
[3] L. Bunimovich and Y.G. Sinai, Spacetime chaos in coupled map lattices, Nonlinearity 1 (1988) 491–516.
[4] H. Chaté, Spatio-temporal intermittency in coupled map lattices, in: T. Riste and D. Sherrington, eds., Spontaneous formation of space-time structures and criticality, 219 (Kluwer Academic, Dordrecht, 1991).
[5] H. Chaté and P. Manneville, Transition to turbulence *via* spatiotemporal intermittency, Phys. Rev. Lett. 58 (1987) 112.
[6] H. Chaté and P. Manneville, Spatio-temporal intermittency in coupled map lattices, Physica D 32 (1988) 409.
[7] H. Chaté and P. Manneville, Structure of clusters generated by spatiotemporal intermittency and directed percolation in two space dimensions, Phys. Rev. A 38 (1988) 4351.
[8] J. Froyland, Some symmetric, dissipative, two-dimensional maps, Physica D 8 (1983) 423–434.
[9] P. Gorá and A. Boyarski, Absolutely continous invariant measures for piecewise expanding C^2 transformations in R^n, Isr. J. Math. 67 (1989) 272.
[10] S. Grossman and S. Thomae, Correlations and spectra of periodic chaos generated by the logistic parabola, J. Stat. Phys. 26 (1981) 481.
[11] V. Gundlach and D. Rand, Spatio-temporal chaos: 1. Hyperbolicity, structural stability, spatiotemporal shadowing and symbolic dynamics, Nonlinearity 6 (1993) 165.
[12] V. Gundlach and D. Rand, Spatio-temporal chaos: 2. Unique Gibbs state for higher dimensional symbolic system, Nonlinearity 6 (1993) 201.
[13] V. Gundlach and D. Rand, Spatio-temporal chaos: 3. Natural spatio-temporal measures for coupled circled map lattices, Nonlinearity 6 (1993) 215.
[14] J. Houlrik, Periodic orbits in a two variable coupled map, Chaos 2 (1993) 397.
[15] A. Ivanov and A. Šarkovskiĭ, Oscillations in singularly perturbed delay equations, Dyn. Rep. 3 (1991) 165.

[16] J.A.C Gallas, P. Grassberger, H.J. Hermann and P. Ueberholz, Noisy collective behavior in cellular automata, Physica D 180 (1992) 19–41.
[17] M. Jakobson, Asbolutely continuous invariant measures for one-parameter famlilies of maps, Commun. Math. Phys. 81 (1981) 39.
[18] J.M. Yuan, M. Yung, D.H. Feng and L. Narducci, Instabilities and irregular behavior in coupled logistic equations, Phys. Rev. A 28 (1983) 1662–1666.
[19] K. Kaneko, Pattern dynamics in spatiotemporal chaos, Physica D 34 (1989) 1.
[20] K. Kaneko, Overview of coupled map lattices, Chaos 2 (1993) 279.
[21] J. Komornik and A. Lasota, Asymptotic decomposition of Markov operators, Bull. Polish Acad. Sci. 35 (1987) 321.
[22] A. Lasota and M. Mackey, Probabilistic Properties of Deterministic Systems (Cambridge Univ. Press, Cambridge, 1985).
[23] E. Lorenz, Noisy periodicity and reverse bifurcation, NY Acad. Sci. 357 (1980) 282.
[24] J. Losson and M. Mackey, Asymptotic periodicity in coupled map lattices, preprint, Phys. Rev. E, submitted.
[25] M. Mackey, Time's Arrow: The Origin of Thermodynamic behavior (Springer, Berlin, 1992).
[26] M. Mackey and U. van der Heiden, The dynamics of recurrent inhibition, J. Math. Biol. 19 (1982) 211.
[27] Y. Pomeau, Periodic behavior of cellular automata, J. Stat. Phys. 70 (1993) 1379–1382.
[28] N. Provatas and M. Mackey, Asymptotic periodicity and banded chaos, Physica D 53 (1991) 295–318.
[29] D. Ruelle, Measures describing a turbulent flow, NY Acad. Sci. 357 (1980) 1–9.
[30] Y.G. Sinai, Construction of Markov partitions, Funct. Anal. Appl. 2 (1968) 245.
[31] H.M. T. Yoshida and H. Shigematsu, Analytic study of chaos of the tent map: Band structures, power spectra and critical behaviors, J. Stat. Phys. 31 (1983) 279.
[32] T. Yamada and H. Fujisaka, Effect of inhomogeneity on intermittent chaos in a coupled system, Phys. Lett. A 124 (1983) 421–425.